Depth estimation of gravity anomalies by S-transform of analytic signal

Mousavi, N.[1*] and Ebrahimzadeh Ardestani, V. [2]

1. Ph.D. Candidate, Institute of Geophysics, University of Tehran, Tehran, Iran
2. Professor, Institute of Geophysics, University of Tehran, Tehran, Iran

Abstract

The S-transform has widely been used in the analysis of non-stationary time series. A simple method to obtain depth estimates of gravity field sources is introduced in this study. We have developed a new method based on the spectral characteristics of downward continuation to estimate depth of structures. This calculation procedure is based on replacement of the Fourier transform with the S-Transform in traditional downward formula. We expect the localized estimation of the depth of anomalies using the S-transform spectrum rather than FFT spectrum. Likewise in the wavelets which don't have a direct relationship with wave numbers, the S-Transform corresponds to wave number instead of scale or pseudo wavenumber. This is the main advantage of using S-transform instead of wavelets. This advantage will lead to easier and more precise calculation of depth estimation. Synthetic examples indicate the usefulness of this method. The method was applied to field examples producing reasonable results comparable to some common methods such as wavelet-based source characterization and Euler deconvolution. It is possible to average the local spectra over the wavenumber axis that leads to the spectrum referenced to position axis. The depth of anomaly can be computed in any point of the profile by using localization of spectrum. Thereby, we can analyze distinguished traces of shallow and deep anomalies while the lateral effects are also considered.

Keywords: Analytic signal, Depth estimation, Gravity data, S-Transform.

1. Introduction

The S-Transform (Stockwell et al., 1996) has been applied in many fields of study such as Medicine (Goodyear et al., 2004), Biomedical Engineering (Senapati and Routray, 2011), and Geophysics (Mansinha et al., 1997; Pinnegar and Mansinha, 2003). This transform like other Time Frequency Representations (TFR) is possible to be generated by different scaling frames. The simultaneous representation of information makes up inadequate spectral components and provides localization of information with time and frequency. In the case of gravity data, we have position instead of time to use wavenumber instead of frequency. They do not have conceptually difference, except in symbol substitution in the formula. With the advantage of fast lossless invertibility of position, to position-wavenumber, S-transform (ST) is very analogous to Fourier transforms (Mansinha et al., 1997).

In the last few years, there has been a growing interest among geoscientists to interpret potential field data in the wavenumber domain and particularly Fourier transforms (Gupta, 1988). Spectrum of data using Fourier transforms (FT) contains information in wavenumber space. Depth and source parameter (geometry and density) estimation via the FT is possible using different techniques (e.g. Odegard and Berg, 1965; Mareshal, 1985; Garcia-Abdeslem, 1995; Maus and Dimiri, 1996). Although FT of the entire trend of data contains information about the spectral components but, for a large class of practical applications, this information is inadequate (Stockwell et al., 1996).

Position-scale and position-wavenumber approaches of TFRs include various groups including continuous wavelet transforms (CWT), discrete wavelet transforms (DWT), discrete stationary wavelet transforms (SWT), and short-time Fourier transforms (STFT). As STFT is not dependent on the

*Corresponding author: E-mail: mousavi_naeim@yahoo.com

wavenumber and has a fixed width for all wavenumbers, it gives poor spatial resolution of high-wavenumber events. In fact, the ST is the STFT with Gaussian windows (or Gabor transformation) which has the variability property rather than fixed windows of STFT. The DWT particularly separates the field into the distinguished components belonging to different scales and horizontal positions. The CWT may characterize the sources (depth, source type) of the separated field effects (Fedi et al., 2004). DWT has been used as a powerful tool in filtering and de-noising.

Wavelet families produce sufficiently the resolved information applicable to spectral analysis of gravity data. Unlike Fourier transforms, Wavelet Transforms ensure position-wavenumber resolution suitable to non-stationary signals like gravity data. The CWT exploits the upward continuation properties of the field horizontal derivative and allows the location of potential field singularities in a simple geometrical manner (Fedi et al., 2004). Fedi et al. (2004) tried to estimate depth values using a joint application of CWT and DWT. Depth values obtained from their proposed method are referenced to the x-axis. Because of scale dependent information, as in scalogram, the method inevitably applies best-fitting lines method which follows a semi-automatic procedure. Li et al. (2013) used scale normalization on the continuous wavelet transforms, and derive the relationships between the depth of a structure and the pseudo-wavenumber. The depth of source can be recovered from tracing the maximal values of the modulus of the complex wavelet coefficients in the CWT-based scalograms as function of the pseudo-wavenumber (Li et al., 2013). Actual depth values are dependent on wavenumbers inversely; meanwhile the pseudo-wavenumber usage, as a substitute for original wavenumbers, makes some approximations. CWT analysis using wavelets based on the horizontal derivatives of simple gravity and magnetic models, can give useful information on the positions and depths of the sources. CWT should be applied to the appropriate order of horizontal derivative of the data and not directly to the data itself. In Cooper's (2006) method, the anomalies are depicted through contour maps in depth profile cross section, but the depth to top or center of bodies are not signified uniquely.

We have used ST of the analytic signal of gravity data along with some plots in order to estimate the minimum depth while depth estimation is carried out by a semi-automatic procedure using numerical calculations and characteristics of downward depths. We rearranged the traditional equation of downward continuation for describing the relation between depths and wavenumbers that led to the generation of an equation for the depth of buried structures in which the Fourier transform was replaced by the S-transform. Regarding the simultaneous presences of both wavenumber and position in TFRs, as in the ST, computed depth values are referenced to the x-axis. Depth values are referenced to the x-axis. The depth estimation via spectral analysis becomes possible through the direct relationship between ST and the wavenumbers. Using analytic signal of the gravity data prevents self-aliasing (Stockwell et al., 1996) occurring along the direction of x-axis. The obtained depth values set up a matrix. Projecting all rows of this matrix to a vector located actually on data acquisition profile, provides depth values referenced only to the x-axis. Depth values that are estimated through analytic signal are not referenced to exact stations located along the x-axis because of the presumed shift for position using a window with nonzero width. We neutralize these effects by averaging depth values obtained along the x-axis. We can only perform the averaging in limited area around the anomaly to reach the depth to body referenced to its position along profile.

In the CWT and ST plots, using half of the S-matrix allows the depiction of potential field sources due to the amplitude and phase spectrums repetition of FT in the mid-profile for real data. However, we need information of the spectrums, including all wavenumbers, from upper and lower parts in order to reconstruct original signal. We use the spectrum regarding all wavenumbers. To demonstrate the efficiency of the ST in estimating depths to gravity structures, the study has initially provided different instances of synthetic and formerly field data. Tendency of the obtained depth values

to center of bodies can be explained as the effect of superposition with various received wavenumber information from overlying depth levels in body.

2. Depth estimation via the S-Transform (ST)

ST is a generalization of the STFT and an extension of the CWT. ST provides wavenumber-dependent resolution while maintaining a direct relationship with the FT spectrum (Stockwell et al., 1996). It provides supplementary information about spectra which is not available from a locally referenced phase, obtained by the CWT (Sahu et al., 2009). The standard form of the original ST is (Stockwell et al., 1996):

$$S(\mu, k) = \int_{-\infty}^{\infty} h(x)\{\frac{|k|}{\sqrt{2\pi}} \times$$
$$\exp[\frac{-k^2(\mu-x)^2}{2}]\exp(-j2\pi kx)\} \, dx \qquad (1a)$$

where S denotes the ST of h, k is the wavenumber, and the quantity μ is a parameter which controls the position of the Gaussian window on the x-axis. Equation (1a) is a general representation of ST. We can also write (Mansinha et al., 1997):

$$S(\mu, k) = A(\mu, k)e^{j\Phi(\mu,k)} \qquad (1b)$$

where $A(\mu, k)$ is the amplitude of S-spectrum and $\Phi(\mu, k)$ is the phase S-spectrum. The phase $\Phi(\mu, k)$ allows the definition of a broadband generalization of instantaneous wavenumber (Stockwell et al., 1996). The window function $w(\mu, k) = \frac{|k|}{\sqrt{2\pi}} \times \exp[\frac{-k^2(\mu-x)^2}{2}]$ is a scalable Gaussian window. ST windows also satisfy the condition (the admissible condition which provides invertibility condition):

$$\int_{-\infty}^{\infty} w(\mu, k) \, d\mu = 1 \qquad (2)$$

One would expect a simple operation of averaging in the local spectra over the x-axis (positions of stations) as to be represented as a function dependent on the wavenumber. In practice, w is replaced by a more detailed window. Equation (3) indicates that the ST is invertible:

$$\int_{-\infty}^{\infty} S(\mu, k) \, d\mu = G(k) \qquad (3)$$

In the wavenumber domain the operation of downward continuation is:

$$G_z(k) = G_0(k)e^{-|k|z} \qquad (4)$$

where $G(k)$ is the Fourier transform of gravity data, k is wavenumber, and z is the downward continuation distance (Blakely, 1995). This formula provides downward continuation of the potential field data at various depths. This equation is established for any downward depth but there is no simultaneous information of positions for computed depths. The downward continuation of gravity data is inherently unstable and requires regularization, iteration or filtering methods to obtain a stable solution (Kern, 2003). Since unstable results come from deep sources, the existence of the fewer wavenumber bands due to deep structure can reduce the instability in solutions. Fortunately, deep portions of a large body form limited wavenumber bands (located at low wavenumber ranges).

Rearranging Equation (4) seeking the variable z is defined as a function of wavenumber. We have:

$$z(k) = -\frac{1}{|k|} \ln \frac{G_z(k)}{G_0(k)} \qquad (5)$$

In this equation, depth values which are wavenumber dependent are not referenced to the x-axis. The ST, as a member of big TFR families, could be substituted with the simple FT operation in Equation (5). Depth values are related to both, the x-axis and the wavenumber axis, as in $S(\mu, k)$. For dividing two vectors we can apply following strategy. Rows of the Matrix of ST have the length (matrix width) equals to the length of x-axis ($m = \text{size}(x)$) digitized at stations (arrays' positions). The length of columns (matrix height) is equals to the maximum wavenumber ($n = \text{size}(k)$) digitized at specific wavenumbers. To divide the two matrices, each row vector (including the transformed gravity field at significant depth or wavenumber) is divided into basis vector (first row of the S-matrix called voice n=0) by an element-by-element product. Second row of division matrix is composed of these arrays: [s(2,1)/s₀(1,1), s(2,2)/s₀(1,2), … , s(2,m)/s₀(1,m)]). This operation is as follows:

$$z(\mu, k) = z(i, j) =$$
$$-\sum_{i=1}^{m} \sum_{j=1}^{n} \frac{k(i)}{|k(i)|} \left(\ln \frac{im(S(i,j))}{im(S_0(1,j))}\right) \qquad (6)$$

This equation prepares depth of the

source in wavenumber space (cross-section) where outputs are related to both, x-axis and wavenumbers which are prepared by $S(\mu, k)$. Dimensionally equalization of Equation (6) needs an equalizer coefficient $(k(i))$ to be added to the right side. Conceptually, to obtain depth values we compute the ratio of reduced effect of field in the surface related to strong field effect in actual location of mass. In practice this ratio is calculated by using imaginary part of analytic signal of S-spectrum which leads to actual depth values. As deconvolution process, one can judge ratios numerically and conclude the intermediate parameter (depth) which causes differences. Distinguishing parameter of ratios is depth of source.

When dealing with a real-valued time series, one can use the analytic signal for localization (Stockwell et al., 1996). This has the result of setting all negative frequencies to zero, and thus there is no self-aliasing. At first, Analytical signal has been defined by Nabighian (1972) to ease the complicated vector nature of the magnetic field. Hence, when we deal with Analytical signal, it is not necessary to bear the vector analysis and its complexity. The amplitude of the analytic signal of the total magnetic field produces maxima over magnetic contacts regardless of the direction of magnetization (Nabighian, 1972). The analytic signal of g(x) (i.e. gravity field) is defined as (Nabighian, 1972):

$$a(x) = \frac{\partial g}{\partial x} - i\frac{\partial g}{\partial z} \tag{7}$$

where $\frac{\partial g}{\partial x}$ and $\frac{\partial g}{\partial z}$ are horizontal and vertical gradients, respectively. These can be calculated from Hilbert transform. The depth values can be estimated by performing the summation over columns of depth matrix (Eq. 6). The sum of these n row vectors is the projection of all voices (row vectors of S-matrix) to x-axis. The obtained depth values are wavenumber independent and are only dependent on the position as follows:

$$z(\mu) = \int_{k_0}^{k_{max}} z(\mu, k)\, dk \tag{8}$$

where k_{max} is the wavenumber with the maximum value.

Gravity anomalies are very sensitive to lateral effects and it is almost impossible to eliminate the effect of lateral masses. The gravity signal of a source is not confined to its location. In synthetic examples, the depth values are shifted due to pseudo presence of lateral bodies. In field examples there are actually some lateral anomalies. Therefore, we extract minimum depth values from all values as if lateral effect of anomalies has been eliminated.

Analogous to forward modeling, we can simulate the massive body by finer elements (e. g. prisms). In 3-D scheme we can focus on just one column which is composed of some overlying prisms. Each prism can provide significant wavelength features in gravity signal. All these information are also available in arrays of columns of S-spectrum (S-matrix) which provide depth of any prism through these formulas (Eq. 10). These depth arrays do not separately represent actual depth to anomaly therefore we have to operate summation on them. We obtain a unique value for depth of whole the column through invertibility property of S-matrix. Uniquely obtained depths can be given as less ambiguous results instead of different depth components computed respect to one surface point. Hence, the flexibility of ST in return to position domain constrains the solution and reduce ambiguities in CWT which is lacking the invertibility.

3. Synthetic examples

In the first example, we compute the gravity effect produced by a cube, buried at a depth 30 m below the datum, with density contrast of 400 kg/m^3, and length 30 m (Fig. 1a). The gravity anomaly is calculated along the profile with a length of 200 m at intervals of 10 m.

The self-aliasing available in the ST of gravity data is disappeared by using the analytic signal of gravity data which can be seen in the map of imaginary part of ST (Figs. 1c and 1d). Regarding the top depth to cube, some of the depth values located near the cube fit well, but other's variances are relatively high.

The averaging of depth values leads to nearly top depth to prism. Using a 5% Gaussian noise, mean depth value calculated near anomaly (Table 1), is still close to the top depth (Fig.1d). This indicates that our method is consistent with noise. The oscillation of depths may be caused due to the non-zero width of window.

The ST is qualified for analysis of non-stationary signals. In the case of existence of an isolated anomaly, the non-stationary property of signal is weak. Existence of two bodies with indifferent depths provides much non-stationary property for the signal. Hence, the depth values, locally referenced to the x-axis, could be achieved. For the second example, the numeric depth spectrum is computed from the gravity anomaly caused by two prisms that are in depths of 20m (left cube) and 45m (right cube) below the datum. The density contrasts of both cubes are 300 kg/m^3. Left cube is a narrow vertical and the right one is wide horizontal one. The gravity effects are shown in Figure 2a.
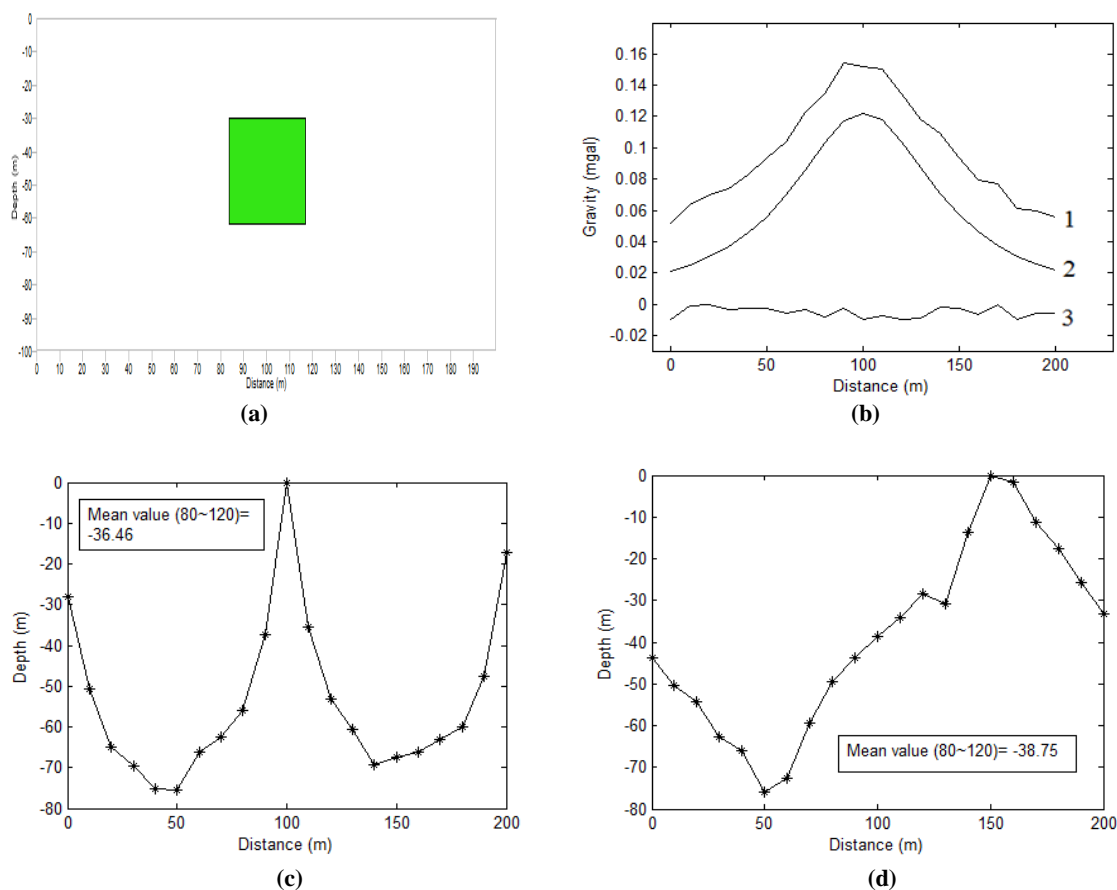
Fig. 1. (a) Synthetic model, (b) Gravity anomaly due to synthetic model. Trace 2 is the pure gravity data. Trace 1 is the data from trace 2 with the addition of 10% of random noise. Trace 3 is the added noise. Trace 1 has been shifted in amplitude by 0.1 units and trace 3 by -0.05 units for better display. (c) Depth values to the analytic signal of pure gravity data, (d) Depth values to the analytic signal of gravity data with 10% noise.

The gravity anomaly is calculated along profile with length of 400 m at an interval of 15 m. All the locally depth values in the specific range of profiles are related to the subsurface structures. Local averaging of depth values along the limited area of profile provides the depths close to top of cubes (Fig. 2d). The obtained Depth values using the S-transform of analytic signal of gravity data are locally referenced to the x-axis. We also offer a unique value for depth rather than what happened in wavelet analysis by Cooper (2006) in which location of structures is estimated visually by using contours in depth cross-sections. The example of his method will be offered in second field example. Based on the results of second synthetic model, we can conclude that in the presence of lateral bodies our method is more accurate than in presence of only one anomaly in estimation of depth to deeper anomalies.

(a)

(b)

(c)

(d)
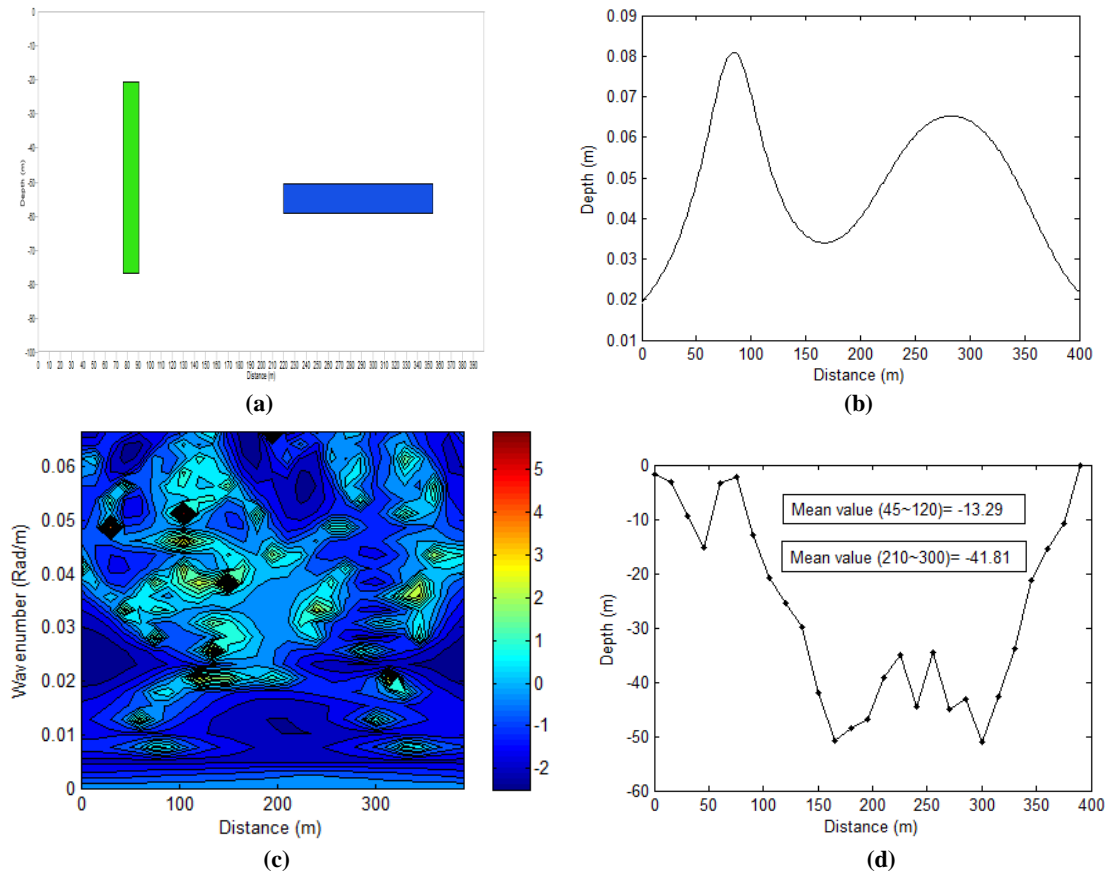
Fig. 2. (a) Synthetic models, (b) Gravity anomaly due to synthetic models, (c) Contour map of depth matrix $z(\mu, k)$ (real values) calculated using Eq. (6) or Eq. (8), (d) Depth values referenced to x-axis using the pure data.

Table 1. Estimated depths and relative errors for synthetic model shown at Fig. 1a in the presense of noise and without noise.

N/S= 0% (ratio of Noise to Signal), minimumdepth= 30		
	Z_{min} (m)	Relative error (m)
Averaging near 80~120	36.46	0.215
N/S= 5%, original depth= 30		
	Z_{min} (m)	Relative error (m)
Averaging near 80~120	38.75	0.291

4. Real data

The first set of real data belongs to the region entitled Cheshmeh-e-Bel (Bel spring), as an underground water conduit (cavity), displayed in Figure 3a, located beside the Sirvan river in the Paveh city, Kermanshah Province of Iran. It is located within 46º, 20´ longitude and 35º, 10´ latitude. Main geological formation in this section is related to Shahoo Bel limestone (Cretaceous time) which is about 0.4 to 2 m thick with irregular bedding. It contains some cherty parts and also karstic and dissolution cavities. Position of cavities was determined using geological information, topography data and eye witnesses in the cavity mouth (Fig. 3a). Our depth estimation can be performed using such isolated negative anomaly where is relying on the profile AB. Depth estimation to an isolated anomaly can be processed effectively through the present method. The location of an anomaly obtained from the available peaks in the curvature (Fig. 3b) is according to the peak in the trend of data.

(a)

(b)

(c)

(d)
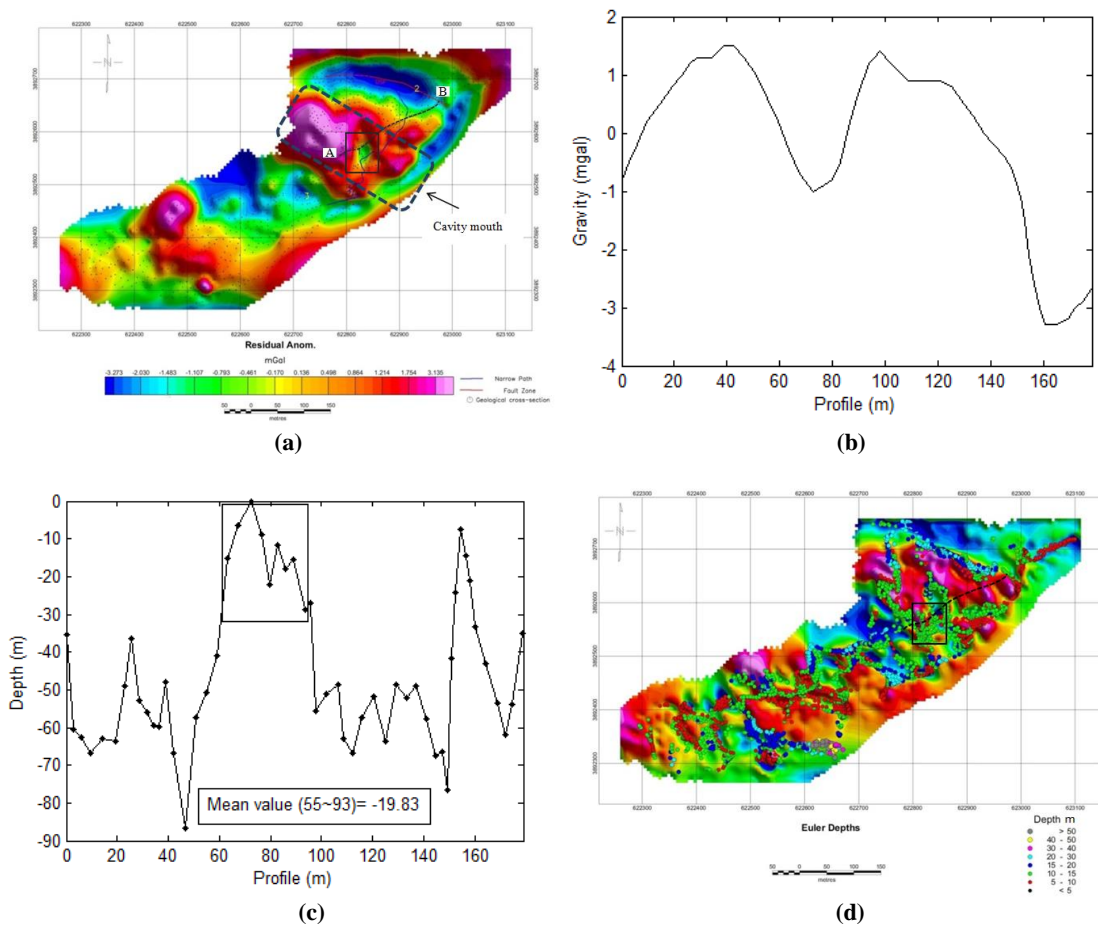
Fig. 3. (a) Residual map of Bel spring, Paveh, Iran. Depth estimation for gravity data related to profile AB is performed. The target negative anomaly is relied at solid line box. Inclined box (dashed line) shows the presumed direction of subsurface tunnel (cavity). (b) Gravity anomaly of data due to profile AB is displayed in Fig. 3a. (c) Depth values plot using ST of the analytic signal of gravity data. Interested area along profile has been shown as in a box. (d) Depth estimation using Euler method. The obtained values for depths (5 to 15 m) are related to top of anomalies (minimum depth).

Obtained depth from our method in the near area to cavity path is 19.83 m. The trace of data is much smoothed; therefore, we expect that the depth values reflex the deeper surfaces rather than top surface. The result shows a close agreement to Euler's depths (5-15 m) computed through Oasis Montaj Software (Fig. 4d). For the purpose of comparison, we apply a result from inverting the profile data. The inversion results have been provided from study by Ardestani (2010). The top depth of conduit is approximately 20 m (Ardestani, 2010, his figures 11 and 12.)

The second set of real data belongs to the area called Safo mining camp in Maku-Iran where is well known for manganese ores and iron-manganese deposits (within sedimentary pelagic rocks and radiolarian cherts). However, the Safo deposit is the viable area for mining

which has been distinguished so far. From geochemistry assessment, Calcite with quartz and barite present as minor phases whereas pyrolusite, bixibite, braunite and hematite are the main minerals, of which the pyrolusite is the dominant ore.

This area is geologically located in the Khoy ophiolite zone, in the northwest Iran. The area of the gravity survey extends between UTM coordinates 438276~438609 west and 4342971~4343187 north. The measurements were corrected for the effects caused by instruments and tidal drift, latitude, free air and the Bouguer correction to yield the Bouguer gravity anomaly (Fig. 4a). The Bouguer anomaly displays extreme magnitudes in the central of the area in the north-south direction, related to mineral occurrence which has high density contrast with the host rocks.

Table 2. Estimated depths and relative errors for left and right cubes shown at Fig. 2a in the presense of noise and without noise.

	top depths of models (m)	Z_{min} (m)	Relative error (m)
Left prism (75~135)	20	13.29	0.335
Right prism (255~315)	45	41.81	0.070

Table 3. Estimated depths and relative errors for conduit at Fig. 3a.

minimum depth from inversion= 20		
	Z_{min} (m)	Relative error (m)
Euler depth	10	0.5
ST	19.83	0.008

(a)

(b)

(c)

(d)
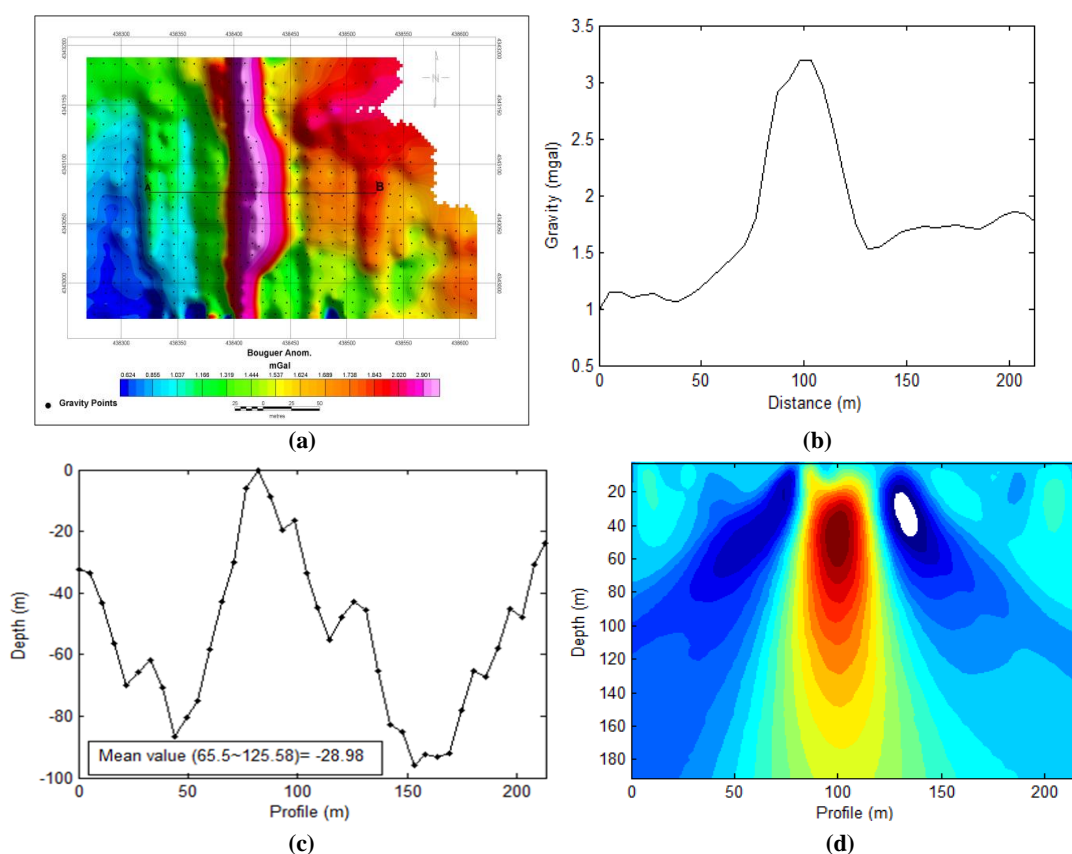
Fig. 4. (a) Bouguer anomalies and the profile AB over the main positive anomaly, (b) Gravity trace along profile AB, (c) Depth values which are plotted versus x-axis using the ST, in which local mean value is equal to minimum depth of ore body, (d) CWT analysis using a wavelet applied to the first horizontal derivative.

To apply the ST-based spectral analysis, profile AB (Fig. 4a) is considered perpendicular to the direction of the main positive anomaly. The mean estimated depth value using the ST is equal to 28.98 m (Fig. 4c). Although by limiting the boundary of averaging this magnitude is decreased. Another method of obtaining location and depth estimates of gravity sources has been suggested by Cooper (2006) who used the continuous wavelet based on the integer-order horizontal derivatives of the gravity anomaly. Our results (ST-based analysis) show a good correlation with Euler and Cooper's results. Nevertheless, when we use S-transform and Wavelet (Figs. 4c and 4d), the depth values are further due to deeper parts of bodies compared with Euler deconvolution (Fig. 4e).

Table 4. Estimated depths and relative errors for mangenese ore at Fig. 4a

	average depth from inversion= 20	
	Z$_{min}$ (m)	**Relative error (m)**
Wavelet analysis	40	1
ST	28.98	0.449

Based on the results from Vatankhah et al. (2013) who used inverse method to obtain the model for storage of manganese ore, the horizontal extension of the obtained model is about 30m and the vertical extension shows a depth interval approximately between 5m and 35m. We could compare the obtained results for approximately top depth from wavelet analysis, and current ST-based method. The comparison results are collected in Table 4.

5. Conclusions

This method is advantageous over the Fourier transform method in downward continuation equation because of S-transform simultaneous representation of spectral information referenced to position space. Using the localization property of the S-Transform, it is more flexible than continuous wavelet transform to compact the wide spread spectral information (referenced to wavenumbers) into a single depth vector representing depth values referenced to position axis (x-axis). Therefore, we can offer a unique value for depth instead of non-unique values (contour maps) represented in depicted anomalies by Continuous Wavelet Transforms. The application of ST in our proposed method provides depth estimation to near surface anomalous structures locally referenced to x-axis, with less non-uniqueness of value for the top depths. However, there are still some ambiguities in exact location of depth values along profile because of non-zero width of S-transform windows.

Regarding the calculated relative errors, the computed depths for either synthetic or field examples indicate that this method is reasonably acceptable. Depth estimation results are on the level of commonly used deconvolution methods. Furthermore, this method requires no priori information about density.

References
Ardestani, E. V., 2010, Delineating and modeling an underground water conduit by scattered micro-gravity data and electrical resistivity sounding, Exploration Geophysics, 41, 210-218.

Blakely, R. J., 1995, Potential theory in gravity and magnetic applications, Cambridge University Press.

Cooper, G., 2004, The stable downward continuation of potential field data, Exploration Geophysics, 35, 260-265.

Cooper, G., 2006, Interpreting potential field data using continuous wavelet transforms of their horizontalderivatives, Computers & Geosciences, 32, 984-992.

Fedi, M. and Florio, G., 2011, Normalized downward continuation of potential fields within the quasi-harmonic region, Geophysical Prospecting, 59(6), 1087-1100;

Fedi, M., Primiceri, R., Quarta, T. and Villani, A. V., 2004, Joint application of continuous and discrete wavelet transform on gravity data to identify shallow and deep sources, Geophysical Journal International, 156, 7-21.

Garcia-Abdeslem, J., 1995, Inversion of the power spectrum from gravity anomalies of prismatic bodies, Geophysics, 60(6), 1698-1703.

Goodyear, B. G., Zhu, H., Brown, R. A. and Ross Mitchell, J., 2004, Removal of phase artifacts from fMRI data using a Stockwell transform filter improves brain activity detection, Magnetic Resonance in Medicine, 51, 16-21.

Gupta, O. P., 1988, A Fourier transform minimization technique for interpreting magnetic anomalies of some two-dimensional bodies, Canadian Journal of Exploration Geophysics, 24(2), 179-184.

Kern, M., 2003, An analysis of the combination and downward continuation of satellite, airborne and terrestrial gravity data, PhD thesis, the university of Calgary, Alberta, Canada.

Li, Y., Braitenberg, C. and Yang, Y., 2013, Interpretation of gravity data by the continuous wavelet transform: The case of the Chad lineament (North-Central Africa), Journal of Applied Geophysics, 90, 62-70.

Mansinha, L., Stockwell, R., G., Lowe, R., P., Eramian, M. and Schincariol, R., A., 1997, Local S-spectrum analysis of 1-D and 2-D data, Physics of the Earth and Planetary Interiors, 103, 329-336.

Mareshal, J. C., 1985, Inversion of potential field data in Fourier transform domain, Geophysics, 50(4), 685-691.

Maus, S. and Dimiri, V., 1996, Depth estimation from the scaling power spectrum of potential fields, Geophysical Journal International, 123, 113-120.

Odegard, O. and Berg, J. W., 1965, Gravity interpretation using the Fourier integral, Geophysics, xxx, 3, 424-438.

Pinnegar, C. R. and Mansinha, L., 2003, The S-transform with windows of arbitrary and varying shape, Geophysics, 68(1), 381-385.

Nabighian, M. N., 1972, The analytic signal of two dimensional magnetic bodies with polygonal cross-section: its properties and use for automated anomaly interpretation, Geophysics, 37, 507-517.

Nabighian, M. N., Ander, M. E., Grauch, V. J. S., Hansen, R. O., LaFehr, T. R., Li, Y., Pearson, W. C., Peirce, J. W., Phillips, J. D. and Ruder, M. E., 2005, Historical development of the gravity method in exploration: Geophysics, 70(6), 63ND-89ND.

Senapati, K. and Routray, A., 2011, Comparison of ICA and WT with S-transform based method for removal of ocular artifact from EEG signals, Journal of Biomedical Science and Engineering, 4, 341-351.

Stockwell, R. G., Mansinha, L. and Lowe, R. P., 1996, Localization of the complex spectrum: the S-transform, IEEE Transactions on Signal Processing, 44, 998-1001.

Vatankhah, S., Ardestani, E. V. and Renaut, R. A., 2013, Automatic estimation of the regularization parameter in 2-Dfocusing gravity inversion: an application to the Safo manganesemine in northwest of Iran, Journal of Geophysics and Engineering (in press).